**MOUNTAIN BY MOUNTAIN: DEFINING LUNAR BASINS** A.M. Bailey, R.V. Wagner, M.S. Robinson.
School of Earth and Space Exploration, Arizona State University, Tempe, AZ 05281, USA (ambail10@asu.edu).

**Introduction:** Surprisingly, the topographic definition of a mountain is not well constrained [1,2]. Terrestrial geology has produced definitions based on remote sensing data which allows application to other planetary bodies. We measured key topographic parameters of lunar mountains, or massifs, from the Lunar Reconnaissance Orbiter Camera (LROC) 100 m/px GLD100 digital terrain model (DTM), merged with a LOLA DTM near the poles [3,4].

The identification of mountains through consistent topographic characterization and statistical analysis enables the discovery and documentation of ancient peak rings in multi-ring impact basins (D > 300 km) [5] and quantitative modeling of basin formation to acquire a better understanding of the significance of lunar massifs. By measuring mountains, we can better understand fundamental structures of the lunar crust [6], and with a consistent set of topographic measurements, we aim to reconstruct basin rings. Initially, basins have crisp mountain chains that define rings, but as they age, the basin rings lose their sharp morphology through creep and impact-induced degradation.

South-Pole Aitken (SPA) basin is the largest confirmed lunar impact basin (2,500 km diameter), and it has a well-preserved outer ring [7]. SPA is thought to be the oldest preserved basin on the Moon: its crater size frequency distribution model age is ~4.3 Ga [8]. Thus, it is a key starting place to measure lunar massifs and give topographic insight to other multi-ring impact basins. We measured mountains surrounding SPA as a preliminary study to establish a methodology to identify lunar mountains and investigate basin rings.

**Methods:** For this study we adapted common terrestrial measurement techniques and parameter definitions to the Moon.

*Terminology:* We define a lunar mountain to have five topographic parameters: elevation, prominence, relief, slope, and maximum relief [**Table 1**]. Any mountain has a parent peak and may contain child peaks. Parent peaks are defined as the peak with the highest elevation for the mountain in question and child peaks (if applicable) are numbered 1–*n* in order of decreasing elevation [**Fig. 1**]. Mountains are subjectively delineated from adjacent mountains based on distance between summits, adjacent mountains may be connected by a low contour but are measured independently [**Fig. 1**].

*Measurement:* For each mountain we recorded base elevation, summit elevation, average relief, topographic prominence of the mountain in question, prominence profiles for parent and child peaks, and maximum relief as defined in **Table 1** and shown in **Fig. 1**.

| | *Measurements, Definition, and Rules* |
|---|---|
| *Summit Elevation* | Highest elevation measured for the mountain in question |
| *Base Elevation* | Lowest elevation measured for the mountain in question. Rule: Boundary around the mountain defined by the leveling off point. Where it levels off without plunging too low or too high in elevation. See **Fig. 1**, white line. |
| *Relief* | Summit elevation – lowest elevation on one profile |
| *Average Relief* | Summit elevation – average base elevation |
| *Maximum Relief* | Summit elevation – lowest possible elevation surrounding it. i.e. the base of an adjacent crater. |
| *Slope* | Rise/run, steepness of summit to base. |
| *Prominence profiles* | The summit elevation to the lowest possible elevation surrounding the individual parent or child peaks in 8 directions (N, NE, E, SE, S, SW, W, NW) to get the significance of the peak itself. [**Fig. 2, 6**] |
| *Topographic Prominence* | The relief of the mountain relative to the lowest encompassing 100 m contour interval that contains no taller peak. See **Fig. 1**, black line. |

***Table 1:*** Definitions as used for this study.

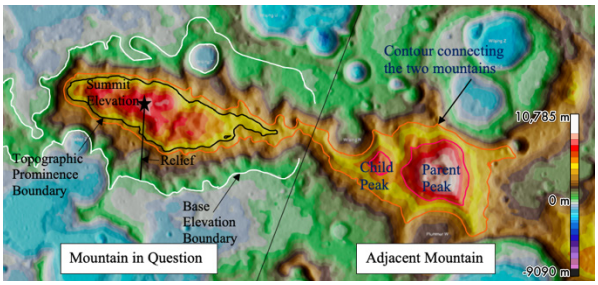


***Fig. 1:*** Definitions in action, example of measurements for a massif at 21.96°S, 201.81°E.

All mountains were measured in six different ways over the merged GLD100/LOLA DTM, to account for changes in relief, as the elevation varies around a peak due to vagaries of surrounding topography [**Fig. 2**]. The six measurements taken are: (1) elevation profile for relief of the mountain in question, (2) elevation profile for topographic prominence, (3) elevation profile for maximum relief, (4) mountain average relief, (5) topographic prominence relief by counting contours, and (6) prominence profiles of parent and child peaks separately **[Fig. 2].** Both LROC Quickmap and local contour maps were used. The SLDEM (Kaguya Terrain Camera + LOLA) was considered but ultimately not used for this study, as measurements did not vary significantly between the GLD100 and the SLDEM at the scales used. Additionally, the SLDEM is only available for 60°S to 60°N latitude [9].

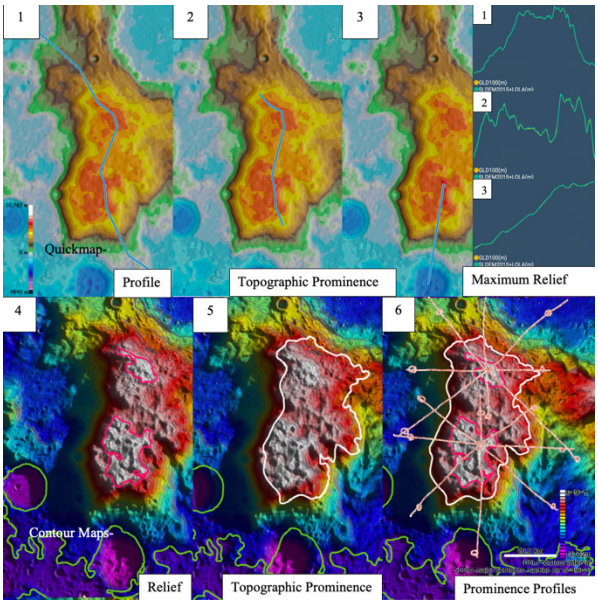


***Fig. 2:*** *1-3* Using the Quickmap elevation profile tool (profiles at top right). *4-6* Contour maps with **pink:** parent and child (not a measurement), **green:** base elevation, **white:** topographic prominence, and **light pink:** prominence profiles for parent and child separately.

**Preliminary Results:** The mountain measured with the greatest relief in the SPA basin (76.92°S, 260.09°E, red star in **Fig. 3**) exhibits an average relief of 8,900 m above its base elevation: more relief above its base than almost any mountain on Earth (Mauna Loa ~9,200 m, Denali ~5,500 m, Mt. Kilimanjaro ~4,900 m, Mount Everest ~4,600 m). Relief around this mountain varies from 5,000 m to 10,400 m as measured by prominence profiles and maximum relief measurements [**Fig. 2 3,6**].

SPA basin has a clear breakdown of mountain types in its surrounding ring. In the north and northeast of the basin [**Fig. 3, quad. 2**] the massifs are closely packed in arcuate groups, while massifs are typically less clustered around the rest of the basin. **Table 2** gives statistics by quadrant, and shows similar relief in all quadrants, but large variations in topographic prominence. This indicates greater clustering of mountains in quadrant 3 (a given mountain is more likely to have a taller neighbor there than elsewhere around SPA), perhaps related to two large craters that seem to interrupt the ring.

*Averages by quadrant + % change from SPA Average*

| | Base Elev. (m) | Summit Elev.(m) | Relief (m) | Topographic Prominence (m) |
|---|---|---|---|---|
| *1* | -780 | 5,430 | 6,200 (+6%) | 2,230 (+4%) |
| *2* | 40 | 5,800 | 5,760 (+1%) | 2,770 (+19%) |
| *3* | -1,800 | 3,930 | 5,730 (+2%) | 1,560 (+33%) |
| *4* | -950 | 4,680 | 5,630 (+3%) | 2,730 (+18%) |
| *SPA* | -872 | 4,960 | 5,830 | 2,322 |

***Table 2:*** Statistics from all 99 measured mountains.

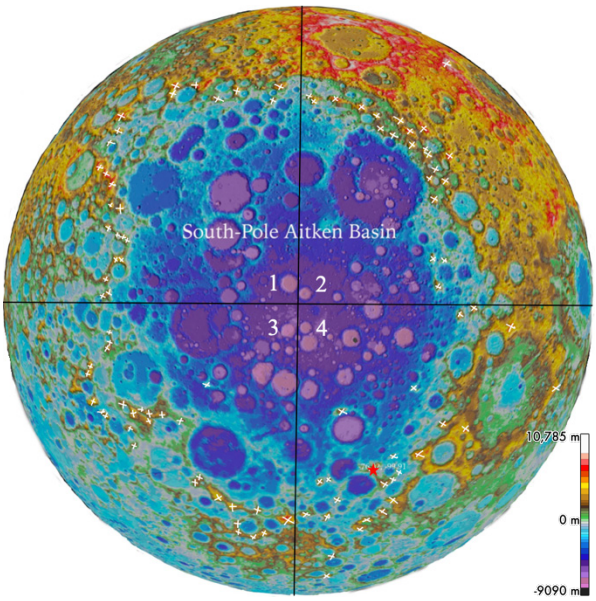


***Fig. 3:*** The SPA Basin, GLD100 color shaded relief map centered on 56.29°S, 193.51°E, split into quadrants. White "x"s indicates measured mountains.

**Discussion:** The morphologic and geographic results of this study document the topographic variation associated with the SPA basin and its rings. While these measurements rely on human judgement to some degree, the rules detailed in **Table 1** minimize uncertainty in mountain-to-mountain comparisons. Identifying lunar massifs is a good indicator for peak ring location and with documented elevation and coordinates, we can estimate where SPA basin rings are more degraded. All six measurements [**Fig. 2**] were used in understanding certain aspects of lunar massifs, (1), (4) and (2), (5) gave similar results, with contour maps best for constraining base elevation and Quickmap the summit elevation, (3) and (6) measured elevation changes. The study of lunar mountains will give further insight into the degradation of multi-ring impact basins and uncover more about the early history of the Moon by helping to establish superposition relationships between basins. To further this investigation, we plan to measure all other lunar basins, measuring to the lunar mean radius to acquire a global elevation range, basin-to-basin comparisons to further understand the variation as it relates to location, and how multi-ring impact basins vary across the Moon.

**References:** [1] Fry et al. (1987) SUMMIT, pp. 16–32. [2] Yamada et al (1999) Earth Surf. Proc.. Landforms, 24(7), pp. 653–660. [3] Scholten et al (2012) JGR, 117(E12), pp. 1–12. [4] Smith et al. (2010) GRL, 37(18). doi: 10.1029/2010GL043751[5] Spudis et al. (1993) Cambridge University Press, 1993, pp. 2–226. [6] Stuart-Alexander et al. (1970) Icarus, 12(3), pp. 440–456.[7] Wilhelms et al (1987) USGS Prof. Paper 1348. [8] Hiesinger et al. (2012) 43rd LPSC #2863. [9] Barker et al (2016) Icarus. 273, pp. 346-355.